A R C H I V E S O F M E T A L L U R G Y A N D M A T E R I A L S
Volume 60 2015 Issue 2
DOI: 10.1515/amm-2015-0203

H. MYALSKA*,♯, K. SZYMAŃSKI*, G. MOSKAL*

MICROSTRUCTURE AND PROPERTIES OF WC-Co HVAF COATINGS OBTAINED FROM STANDARD, SUPERFINE AND MODIFIED BY SUB-MICROMETRIC CARBIDE POWDERS

MIKROSTRUKTURA I WŁAŚCIWOŚCI POWŁOK WC-Co NATRYSKIWANYCH METODĄ HVAF, OTRZYMYWANYCH Z PROSZKÓW STANDARDOWYCH, DROBNOZIARNISTYCH ORAZ MODYFIKOWANYCH SUBMIKROMETRYCZNYMI PROSZKAMI WĘGLIKÓW

In this paper, microstructure and some properties of various coatings based on WC-Co obtained by the High Velocity Air Fuel technique are discussed. Initially, two WC-Co 83-17 powders of standard and superfine size were examined as a feedstock for a coatings deposition on a steel substrate. A standard Amperit 526.074 powder and an Inframat superfine powder were applied. Then three different sub-micrometric powders, WC, Cr_3C_2 and TiC were applied to modify the microstructure of WC-Co (Amperit 526.074). The aim of the investigations was to compare the microstructure and basic properties of coatings deposited from different components. The influence of sub-micrometric additions on mechanical properties of basic coatings was analyzed. Microstructure characterization of powders by using SEM and characterization of their technological properties as well, are presented. For all manufactured coatings obtained by a High Velocity Air Fuel method, the microhardness, porosity, adhesion to a substrate, and fracture toughness were determined. An improvement in WC-Co coating properties, as a result of sub-micrometric carbides addition, was revealed.

Keywords: wear resistant coatings, WC-Co carbide, sub-micrometric carbide, HVAF

W pracy zostały omówione niektóre właściwości oraz mikrostruktura powłok typu WC-Co otrzymywanych metodą naddźwiękowego natrysku cieplnego w atmosferze powietrza (High Velocity Air Fuel). Początkowo, analizowano dwa proszki typu WC-Co 83-17 o standardowym rozmiarze ziarna oraz drobnym ziarnie pod kątem osadzania powłok na podłożu stalowym. Zastosowano standardowy proszek Amperit 526.074 oraz proszek drobnoziarnisty Inframat. Następnie trzy proszki submikrokrometryczne WC, Cr_3C_2 oraz TiC zastosowano w celu zmodyfikowania mikrostruktury proszku WC-Co (Amperit 526.074). Celem badań było porównanie mikrostruktury i różnych właściwości powłok natryskiwanych cieplnie z różnych proszków. Analizowano wpływ dodatków submikrometrycznych na właściwości mechaniczne powłok podstawowych. Scharakteryzowano morfologię proszków przy użyciu mikroskopu skaningowego oraz scharakteryzowano ich właściwości technologiczne. Dla wszystkich wytworzonych powłok uzyskanych za pomocą metody natrysku naddźwiękowego określono mikrotwardość, porowatość, przyczepność do podłoża i odporności na kruche pękanie. Ujawniono poprawę właściwości powłok WC-Co w wyniku wprowadzenia dodatków węglików submikrometrycznych.

1. Introduction

Thermal spray coatings have achieved a popularity due to their unique wear resistance and the weight reduction of structural elements [1, 2]. Carbide thermal sprayed coatings belong to that group and are widely applied for surface modification [2, 3]. In these coatings, good ability for bonding between the hard phases such as WC, Cr_3C_2 or TiC and a ductile metal matrix such as Co or NiCr are created [3, 4]. The mixture of WC-Co powders is primarily used as a hard facing coating with good wear and shock resistance up to 425°C. At higher temperatures, WC decomposes [5], which leads to the decrease of wear resistance [6, 7].

In order to prepare WC-based coatings with a dense structure, high velocity thermal spraying techniques are used. The high velocity air fuel technique (HVAF) is a similar process to the high velocity oxygen fuel technique (HVOF), but instead of an oxygen atmosphere, compressed air is applied. Applying air during the HVAF process reduces costs compared to the oxygen used in HVOF. Additionally, nitrogen is used to feed and accelerate powders, that also enables the decrease of process temperature. Therefore, no oxidation atmosphere exists during thermal spraying and thus avoids the grain growth and oxidation of fine powders [8, 9].

According to the literature [10-13], the reduction of WC grain size, to the nanometer range, leads to an increase of hardness, fracture toughness and wear properties of sintered WC-Co composites. The improvement of properties occurs, because with the carbide grain size decrease, the mean free path of the Co matrix is reduced, which results in an increase

* SILESIAN UNIVERSITY OF TECHNOLOGY, INSTITUTE OF MATERIALS SCIENCE, 8 KRASINSKIEGO STR., 40-019 KATOWICE, POLAND
♯ Corresponding author: hanna.myalska@polsl.pl

of hardness, according to the Hall-Petch relationship and an increase of fracture toughness, due to a greater amount of plastic deformation without cracking. Effects observed in sintered WC-Co composites seem to provide an opportunity for testing in coating deposition technology. According to the work of E.A. Levashov et al. [14], a deposition of wear resistant composite coatings strengthened by nano- or sub-micrometric powders can be realized using different surface engineering techniques.

In this paper, the influence of sub-microcrystalline additions on microstructure and the properties of WC-Co coatings deposited with thermal spraying are examined. For the HVAF method, standard WC-Co and superfine WC-Co powders were used as base components. Sub-microcrystalline WC, Cr_3C_2 and TiC powders were then added to the standard WC-Co. The aim of this study is to examine the possibility of porosity reduction, microstructure uniformity improvement, and the hardness increase of fabricated coatings.

2. Experiment

In order to deposit WC-Co coatings with different sub-micrometric additions, a HVAF technique was applied. In the experiment, we used the standard Amperit 526.074 WC-Co powder with a composition of 83 wt. % WC – 17 wt. % Co and the same powder with addition of WC, Cr_3C_2, TiC respectively. In addition, the WC-Co superfine powder Inframat of Infralloy^{TM} S7400 category was deposited without any additions. The sub-micrometric powders were applied to modify the microstructure and properties of standard WC-Co coating.

To characterize feedstock powders used for coatings fabrication, different methods were applied. An average agglomerate size was determined by a laser diffraction sizer method (Mastersizer Hydro 2000S Malvern Inc.), the density was measured with a pycnometer and the tap density, by Scott's volume method. The microstructure of carbide powders and an element map using the energy dispersive X-ray spectroscopy (EDS) system were observed with a HITACHI S-4200 scanning electron microscope.

The WC-Co standard powder with a sub-micrometric carbides application, was blended in a weight ratio 95-5 before HVAF deposition. The basic HVAF parameters are shown in the Tab. 1. Microstructure characterization of the obtained coatings was carried out with a Nikon Eclipse MA 200 light microscope and with a HITACHI S-4200 scanning electron microscope. The surface distribution of elements was performed using HITACHI S-4200 equipped with EDS Thermo NORAN (System Seven), with 3000 magnification. Coatings porosity was estimated on cross-sectioned samples by quantitative evaluation with Met-Ilo software using SEM images. Coatings micro-hardness was also determined on cross-sectioned samples by the Vickers method with a Micro-hardness Tester FM-800 under load of 100 g. At least 10 indentations were conducted on each coating cross section.

The fracture toughness measurements were provided by an indentation method with a Vickers indenter and the Palmqvist indentation model [15-17] was applied to compute a value of stress intensity factor K_{Ic}.

TABLE 1

Parameters of coatings deposition

		HVAF
Oxygen	Presure[bar]	-
	Flow[l/min]	-
Propane	Presure[bar]	8.5
	Flow[l/min]	75
Air	Presure[bar]	9.2
	Flow[l/min]	85
Nitrogen	Presure[bar]	8.4
	Flow[l/min]	30
Powder feed rate [rpm]		3-7
Surface speed [mm/s]		500

Indentations were made along the mid-plane of the coating and the intender was located such that the two intent diagonals were parallel and perpendicular [16-18].The stress intensity factor K_{Ic} was calculated by measuring the length of micro-cracks produced by the indenter.

To calculate fracture toughness, the following equation was used (Eq.1) [15-20]:

$$K_{IC} = 0.079\left(\frac{P}{a^{\frac{3}{2}}}\right)\log\left(\frac{4.5a}{c}\right) \quad (1)$$

where: P is the applied indentation load (N), a the indentation half diagonal (m), c the crack length from the centre of the indent (m). The applicability limits of this equation are $0.6 \leqslant c/a < 4.5$. In the experiment, the loading force was 10 kg and the fracture toughness was evaluated on the basis of the indentation of the half diagonal and crack length measurements (Fig. 1.).

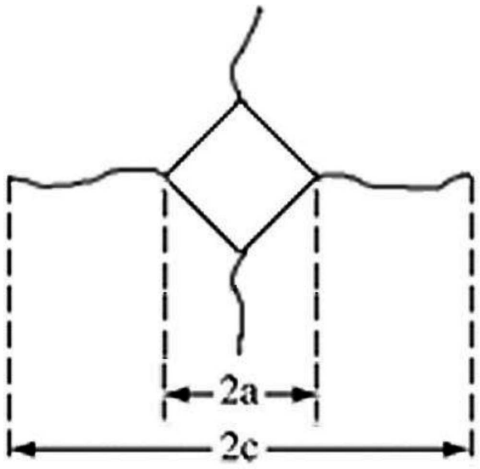

Fig. 1. Schematic of the Vickers indentation used for the fracture toughness determination

3. Results

Results of the initial carbide powder density measurements used for coatings fabrication are shown in Tab. 2. The highest pycnometric density, 15.78 g/cm^3, was found to be

TABLE 2

Densities of initial carbide powders

Powder	WC-Co 83-17 standard	WC-Co 83-17 superfine	Cr_3C_2	TiC	WC
Pycnometric density [g/cm^3]	14.62±0.23	13.65±0.22	-	5.31±0.45	15.78±0.98
Tap density [g/cm^3]	5.92±0.13	5.42±0.11	1.40±0.10	0.35±0.04	1.10±0.15

TABLE 3

Average grain size of carbide powders applied for coatings fabrication

Powder	WC-Co 83-17 standard	WC-Co 83-17 superfine	Cr_3C_2	TiC	WC
Average grain size [μm]	32	28	-	2	9

for sub-micrometric WC. The lowest value of 5.31 g/cm^3 was found for TiC. The assignation of Cr_3C_2 powder pycnometric density was not possible because the powder flow rate was very low. The tap density measurements showed the highest value for WC-Co 83-17 standard powder and it was estimated at 5.92 g/cm^3, also high density value was determined for WC-Co 87-13 superfine powder and it was 5.42 g/cm^3. The value of TiC tap density was the lowest and came to 0.35 g/cm^3.

The results of our average grain size measurements by a laser diffraction method are presented in Tab. 3. The highest average agglomerate size (32 μm) was determined for WC-Co standard powder. The particles of TiC were significantly finer and their average grain size was determined as 2 μm. The mean agglomerates size of WC sub-micrometric powder was at the level of 9 μm.

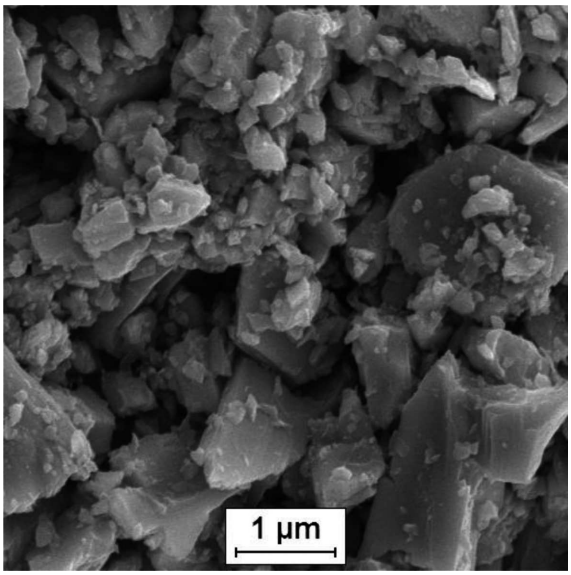

Fig. 2. SEM image of Cr_3C_2 particles

The morphology of the investigated particles observed by SEM was varied. Particles of Cr_3C_2 were irregular with sharp edges (Fig. 2) and a tendency for agglomeration was not observed. The sub-microcrometric TiC powder also revealed no tendency for agglomeration but its particles were globular and finer (Fig. 3). Observations of sub-microcrystalline WC, WC-Co 83-17 standard and WC-Co 83-17 superfine powder (Fig. 4-6) showed evident tendency for agglomeration. The agglomerates of sub-micrometric WC powder were built of globular fine particles, while agglomerates of WC-Co standard and WC-Co superfine consisted of irregular ceramic particles surrounded by cobalt.

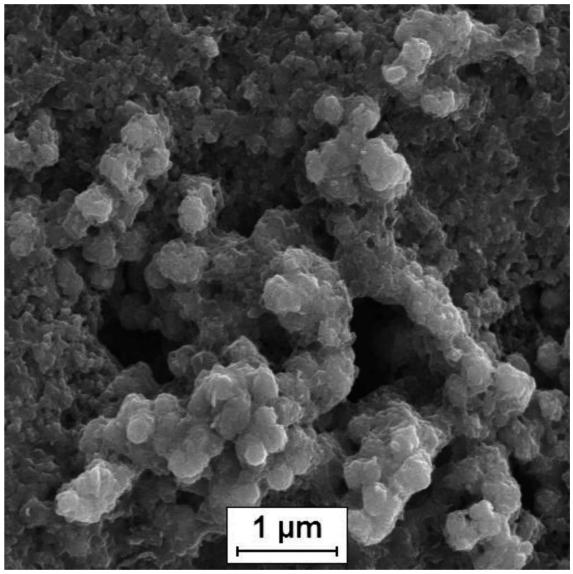

Fig. 3. SEM image of TiC particles

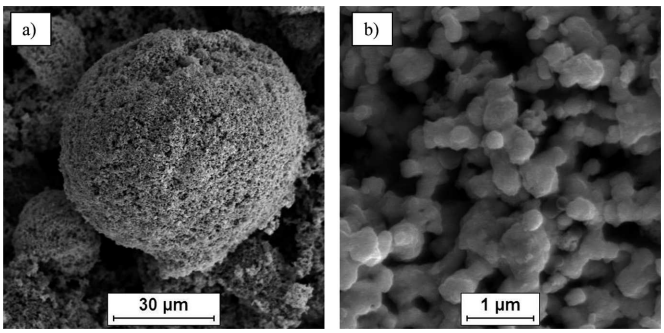

Fig. 4. SEM image of WC powder, a) agglomerate, b) particles

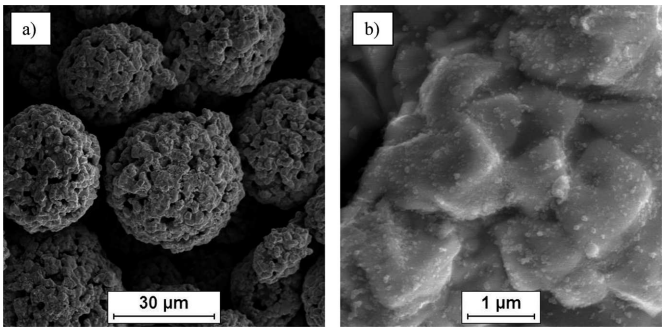

Fig. 5. SEM image of WC-Co standard powder, a) agglomerates, b) particles

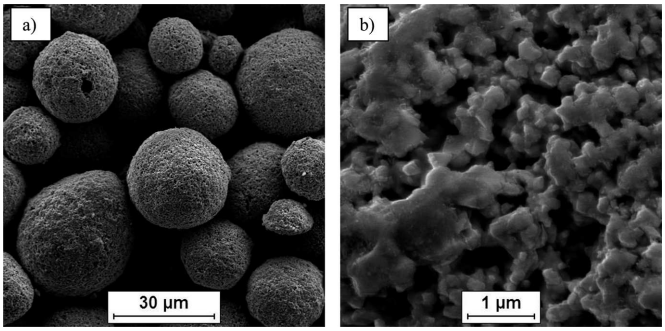

Fig. 6. SEM image of WC-Co superfine powder, a) agglomerates, b) particles

The results of microstructure observations of the obtained coatings carried out with a light microscope and scanning electron microscope are shown in Fig. 7-11. For all deposited coatings, a continuous bonding with a steel substrate was observed by LM, but better effects were obtained for coatings with sub-micrometric additions. The best quality ensured an addition of sub-micrometric Cr_3C_2 and TiC due to an absence of micro-pores and micro-cracks in a thermal sprayed coating – substrate bonding region.

The SEM observations of investigated materials showed that in the coating formed from a standard WC-Co powder, the WC grains of the diameter less than 1.5 μm are uniformly distributed in a cobalt matrix. In the case of the coating obtained from WC-Co superfine powder, the WC grains were uniformly distributed in a cobalt matrix also (Fig. 8b). In the applied magnification, using a secondary electron mode (SE), no distinct differences in microstructure of coatings deposited from mixtures of standard WC-Co powder with sub-micrometric additions were revealed.

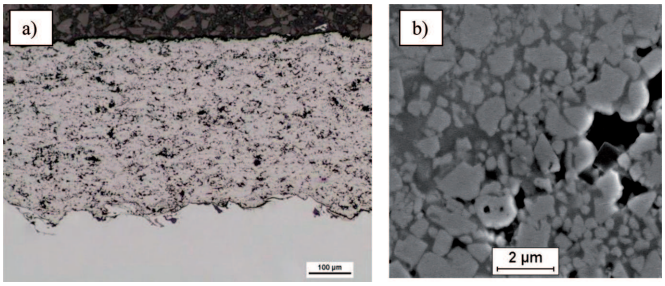

Fig. 7. Microstructure of the coating cross section deposited from WC-Co 83-17 standard powder

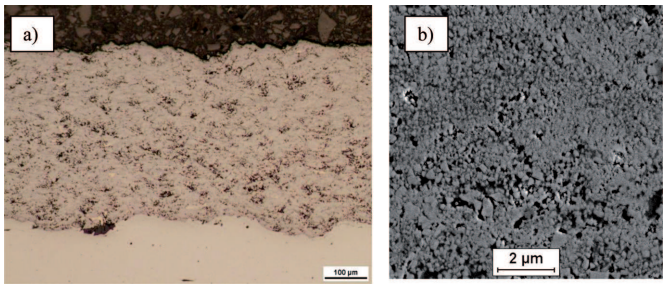

Fig. 8. Microstructure of the coating cross section deposited from WC-Co 83-17 superfine powder

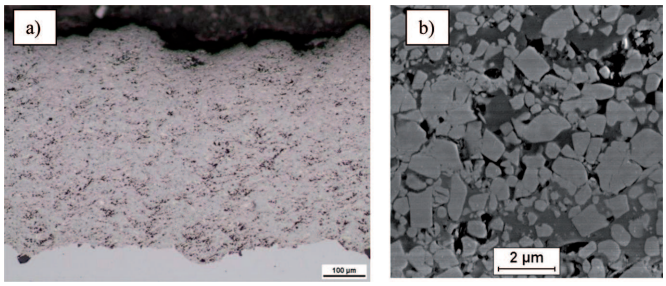

Fig. 9. Microstructure of the coating cross section deposited from a mixture of WC-Co 83-17 standard powder and Cr_3C_2

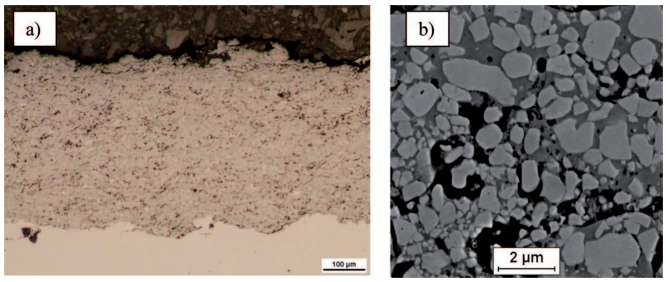

Fig. 10. Microstructure of the coating cross section deposited from a mixture of WC-Co 83-17 standard powder and TiC

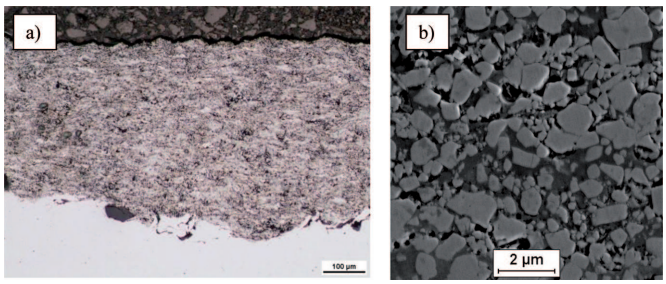

Fig. 11. Microstructure of the coating cross section deposited from a mixture of WC-Co 83-17 standard powder and WC

Basic properties of deposited coatings are presented in Table 4. Despite similar technological parameters of deposition coatings, different thickness was obtained. The thinnest coating of 397 μm was formed from a standard WC-Co, while the thickest coating was obtained from a mixture of standard WC-Co with sub-micrometic Cr_3C_2 addition and its value was estimated at 522 μm. A high thickness (496 μm) was also noticed for the coating deposited from a mixture of standard WC-Co with sub-micrometric WC. For standard WC-Co, superfine WC-Co and a mixture of standard WC-Co with TiC,

the values of the deposited coatings thickness were 397 μm, 431 μm and 444 μm respectively.

The quantitative microstructure description provided by the coatings cross-section images, revealed a significant difference in porosity, dependent on the coatings type. Obtained results of porosity measurements are shown in Table 4. The highest porosity (2.6%) was revealed for a coating from the standard WC-Co powder. The porosity of a coating deposited from superfine WC-Co was 0.6%. The lowest porosity was estimated for a coating obtained from a mixture of standard WC-Co with sub-micrometric TiC powder and it was estimated at 0.5%. Porosity of coatings formed from standard WC-Co with sub-microcrystalline Cr_3C_2 and standard WC-Co with sub-micrometric WC were 0.9% and 1.3% respectively.

The results of micro-hardness measurements revealed a high hardness of thermally sprayed coatings (Tab. 4.). The lowest micro-hardness, 1082 HV0.1, was recorded for coatings deposited from a mixture of standard WC-Co powder with addition of Cr_3C_2. With the addition of TiC and WC sub-micrometric powders to standard WC-Co, an increase of coating micro-hardness was observed. For coatings formed from standard WC-Co with additions of TiC and WC, a minor increase was noticed and the values were 1162 HV0.1, and 1195 HV0.1 respectively. A coating deposited from superfine 83-17 powder was found to have the highest micro-hardness and it was 1374 HV0.1.

The results of slected elements mapping using EDS technique are shown in Fig. 12-16. Uniform distribution of carbon for all deposited coatings was revealed. Also uniform distribution of tungsten was observed for coatings deposited from

TABLE 4

Properties of deposited coatings

	Powder mixture composition				
	WC-Co 83-17 standard	**WC-Co 83-17 superfine**	**WC-Co 83-17 standard + Cr_3C_2**	**WC-Co 83-17 standard + TiC**	**WC-Co 83-17 standard + WC**
Thickness [μm]	397±46	431±18	522±31	444±50	496±74
Porosity [%]	2.6±0.1	0.6±0.1	0.9±0.1	0.5±0.1	1.3±0.1
Hardness [HV0.1]	1129±44	1374±85	1082±56	1162±42	1195±63

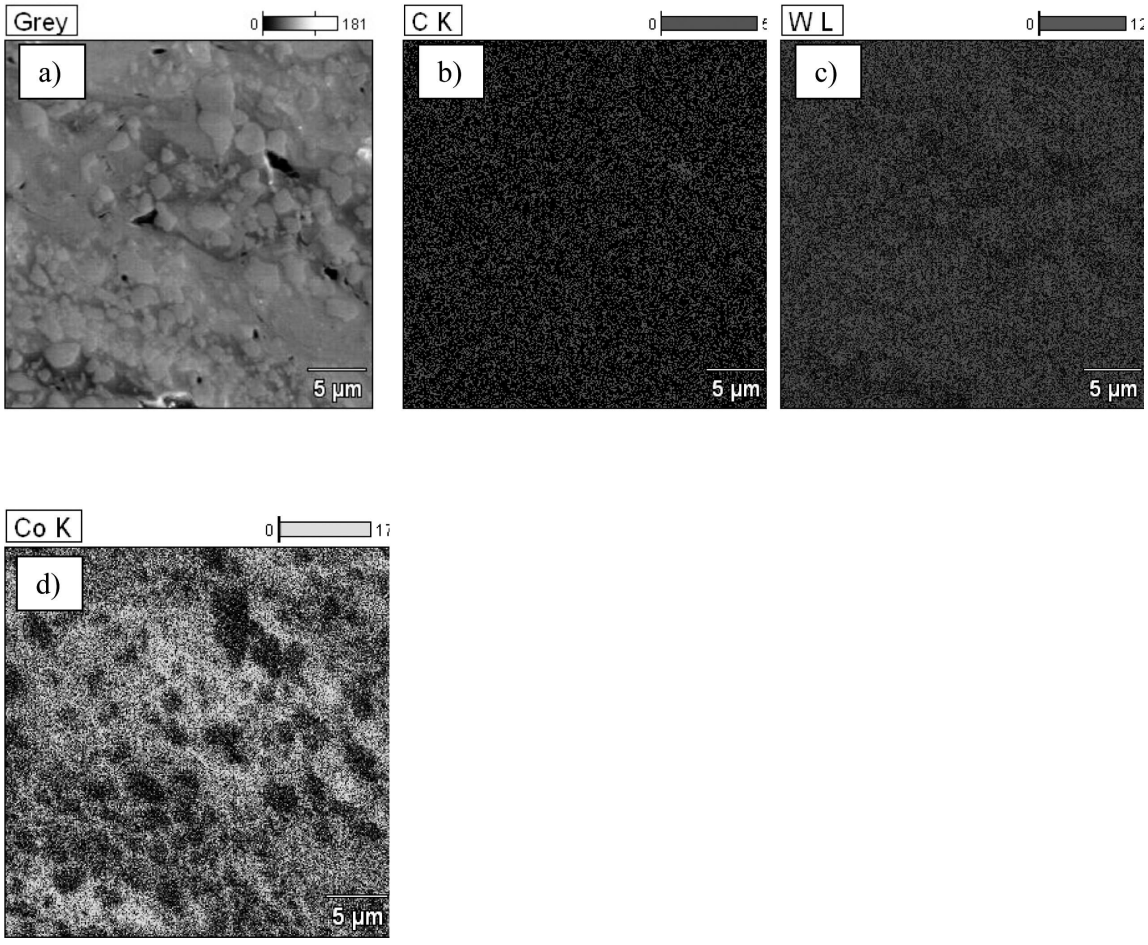

Fig. 12. SEM image (a) and EDS elemantal map images of carbon (b), tungsten (c) and cobalt (d) of the coating deposited from a WC-Co standard powder

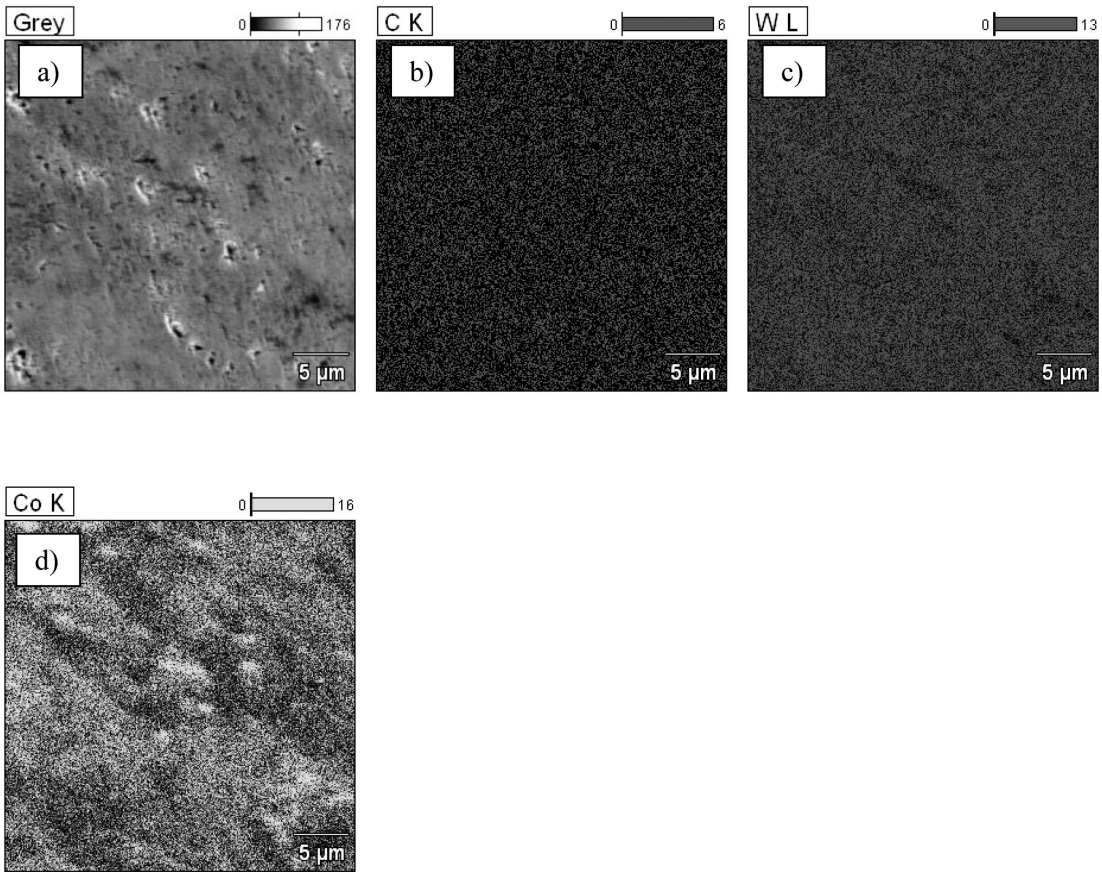

Fig. 13. SEM image (a) and EDS elemantal map images of carbon (b), tungsten (c) and cobalt (d) of the coating deposited from a WC-Co suprefine powder

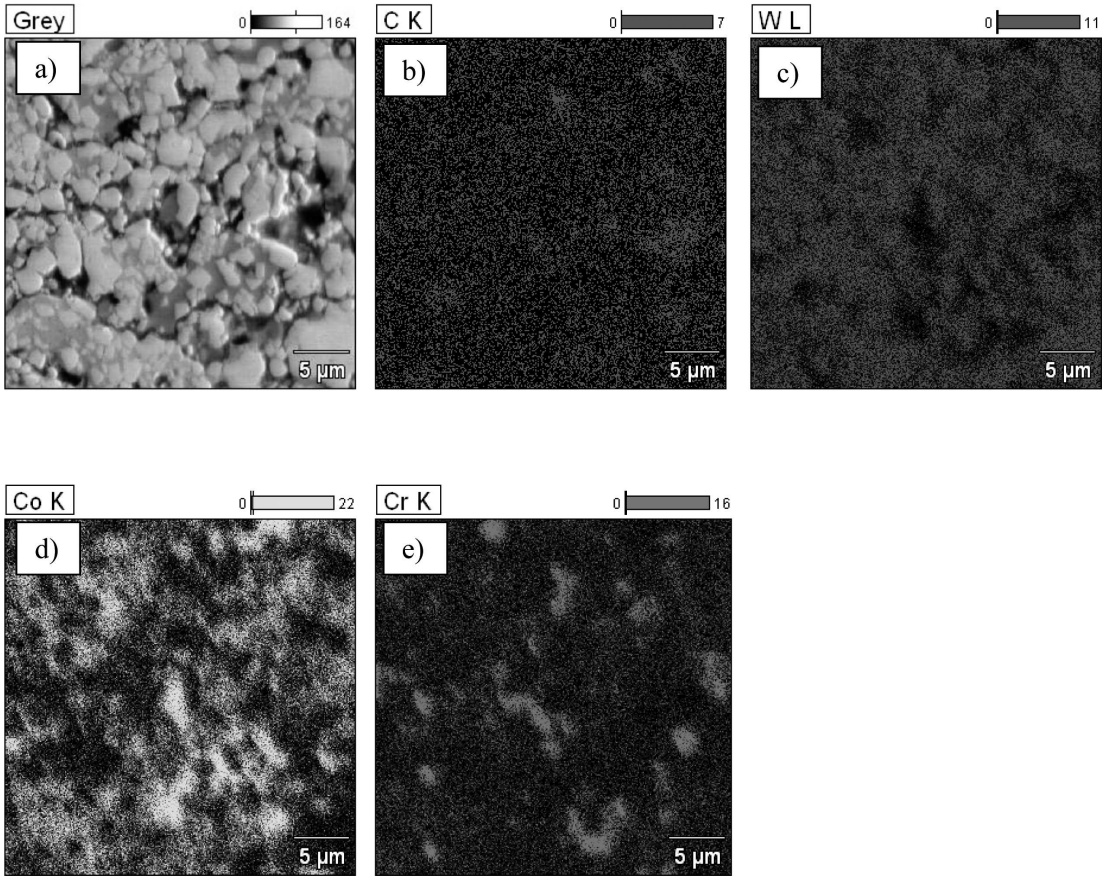

Fig. 14. SEM image (a) and EDS elemantal map images of carbon (b), tungsten (c), cobalt (d) and chomium (e) of the coating deposited from a mixture of WC-Co standard powder and Cr_3C_2 powder

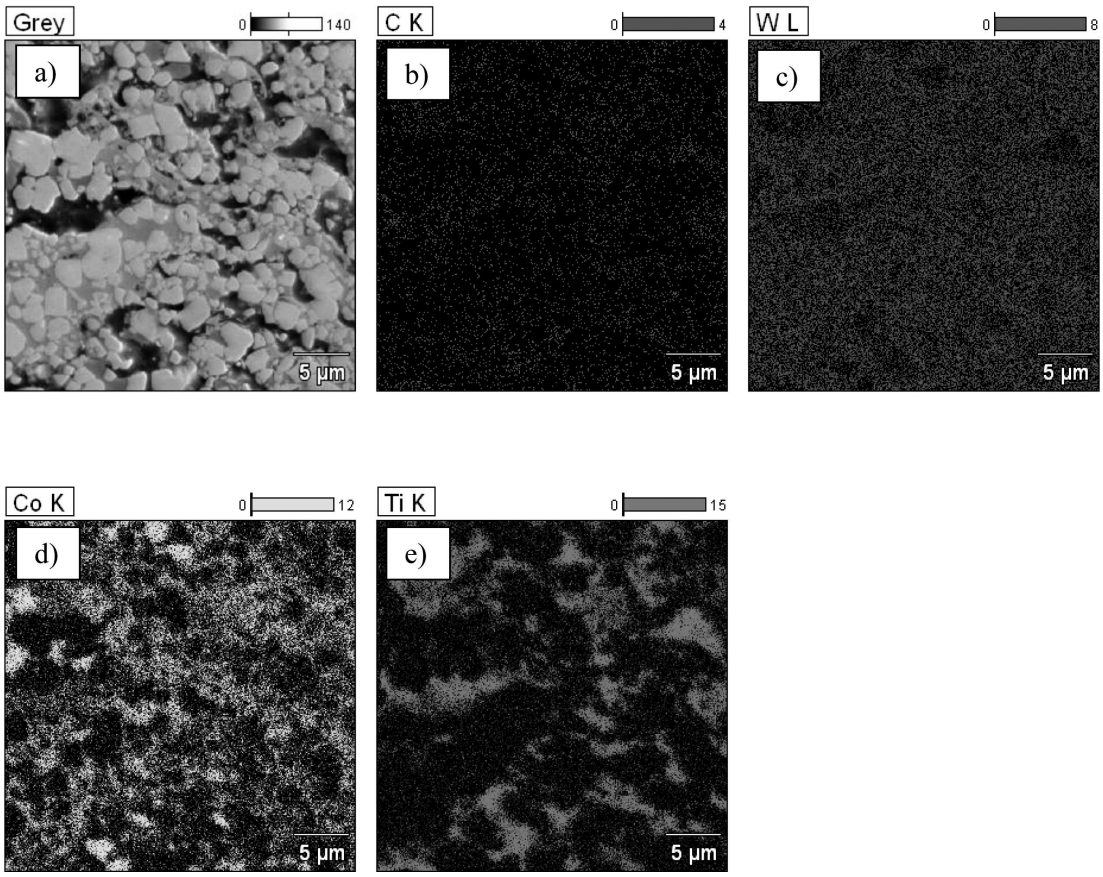

Fig. 15. SEM image (a) and EDS elemantal map images of carbon (b), tungsten (c), cobalt (d) and titanium (e) of the coating deposited from a mixture of WC-Co standard powder and TiC powder

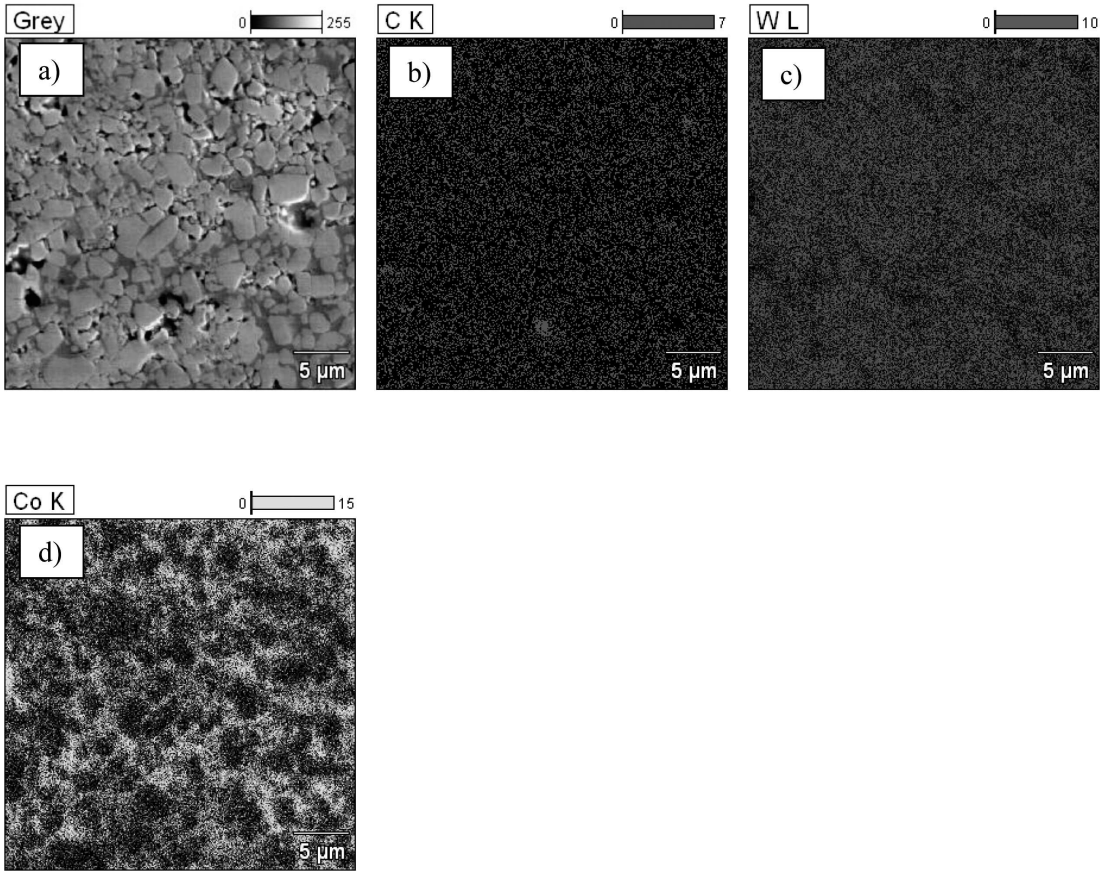

Fig. 16. SEM image (a) and EDS elemantal map images of carbon (b), tungsten (c) and cobalt (d) of the coating deposited from a mixture of WC-Co standard powder and WC powder

TABLE 5

Results of indentation fracture toughness measurements of deposited coatings

	Powder mixture composition				
	WC-Co 83-17 standard	**WC-Co 83-17 superfine**	**WC-Co 83-17 standard + Cr_3C_2**	**WC-Co 83-17 standard + TiC**	**WC-Co 83-17 standard + WC**
Fracture toughness [MPa·m$^{-1/2}$]	1.58±0.61	0.44±0.08	0.43±0.08	0.37±0.16	0.32±0.13

standard WC-Co powder, superfine WC-Co and from the mixture of WC-Co and WC. Cobalt was present mostly in the matrix (darker grey areas). The mapping of elements revealed a presence of chromium and titanium in the coatings deposited from the mixtures of WC-Co with Cr_3C_2 and WC-Co with TiC. During the investigation the darkest areas in the SEM images shown in Fig. 14 and Fig. 15 occurred zones enriched with chromium or titanium. The enriched zones of titanium and chromium probably indicate diffusion of those elements into cobalt matrix. Thus, there is a high probability of a reaction, which occurred between matrix and sub-micrometric powders. The influence of TiC sub-micrometric powder on coating phase composition was confirmed in previous investigation [21].

The results of indentation fracture toughness measurements for fabricated coatings are shown in Table 5. They show significant differences, depending on coating type. The standard WC-Co coating exhibited the highest value of the fracture toughness and it was calculated as 1.58 MPa·m$^{-1/2}$. For the coating deposited from superfine WC-Co 83-17 powder and standard WC-Co with sub-micrometric Cr_3C_2, TiC and WC, the values were 0.44 MPa·m$^{-1/2}$, 0.43 MPa·m$^{-1/2}$, 0.37 MPa·m$^{-1/2}$and 0.32 MPa·m$^{-1/2}$ respectively.

4. Conclusions

The presented research has focused on the modification of a standard WC-Co powder in order to fabricate wear resistant coatings by the HVAF method. Two concepts of coating microstructure changes were proposed. One of them was to apply a powder of the same phase composition (WC-Co) but with significantly finer grain size. The other was to introduce the different sub-microcrystalline carbides to standard WC-Co powder.

Obtained results can be characterized as follows:

– In all applied versions of the HVAF process, good adhesion of coatings to a steel substrate were obtained, independent of a powder type.
– An application of WC-Co superfine powder instead of standard WC-Co powder resulted in a coating porosity and fracture toughness decrease and an increase of micro-hardness.
– The addition of sub-micrometric WC to a standard WC-Co powder generated a decrease of indentation fracture toughness without significant coating porosity and micro-hardness changes.
– Sub-micrometric carbides Cr_3C_2 and TiC used as components with standard WC-Co powder induced a decrease of coatings porosity and fracture toughness, and an increase of micro-hardness.

Acknowledgements

Financial support of Structural Funds in the Operational Program – Innovative Economy (IE OP) financed from the European Regional Development Fund – Project No POIG.0101.02-00-015/09 is gratefully acknowledge.

REFERENCES

[1] G. Barbezat, Surf. Coat. Technol. **200**, 1990 (2005).
[2] L. Thakur, N. Arora, R. Jayaganthan, R. Sood, Applied Surface Science **258**, 1225 (2011).
[3] S. Economou, M. De Bonte, J.P. Celis, R.W. Smith, E. Lugscheider, Wear **220** , 34 (1998).
[4] J. Fochl, T. Weissenberg, J. Wiedermeyer, Wear **130**, 275 (1989).
[5] S.N. Basa, V.K. Sarin, Materials Science and Engineering A **209**, 206 (1996).
[6] M.W. Richert, A. Mazurkiewicz, J.A. Smolik, Arch. of Metal. and Mat. **57**, 2 (2012).
[7] J.A. Smolik, Arch. of Metal. and Mat. **57**, 3 (2012).
[8] A.P. Wang, Z.M. Wang, J. Zhang, J.Q. Wang, Journals of Alloys and Compounds **440**, 225 (2007).
[9] L. Shenglin, S. Dongbai, F. Zishaun, Y. Hong-ying, M. Hui-min, Surf. Coat. Technol. **202**, 4893 (2008).
[10] H.E. Exner, Int. Met. Rev. **4**, 149 (1979).
[11] H. Jianhong, M. Ice, S. Dallek, E.J. Lavernia, Metall. Mater. Trans. A **31**, 541 (2000).
[12] K. Jia, T.E. Fischer, Wear **203-204**, 310 (1997).
[13] B.H. Kear, L.E. McCandlish, Nanostruct. Mater. **3**, 19 (1993).
[14] E.A. Levashov, A.E. Kudryashov, P.V. Vakaev, D.V. Shtansky, O.V. Malochkina, F. Gammel, R. Suchentrunk, J.J. Moore, Surf. Coat. Techn. **180-181**, 347 (2004).
[15] M.M. Lima, C. Goday, P.J. Momodenesi, J.C. Avelar-Batista, A. Davison, A. Mathews, Surf. Coat. Techn. **177-178**, 489 (2004).
[16] C.B. Ponton, R.D. Rawlings, Mater. Sci. Technol. **5** , 865 (1989).
[17] C.B. Ponton, R.D. Rawlings, Mater. Sci. Technol. **5** , 961 (1989).
[18] E. Cantera, B.G. Mellor, Materials Letters **37**, 201 (1998).
[19] L. Fedrizzi, L. Valentinelli, S. Rossi, S. Segna, Corrosion Science **49**, 2781 (2007).
[20] C.W. Lee, J.H. Han, J. Yoon, M.C. Shin, S.I. Kwun, Surf. Coat. Techn. **204**, 2223 (2010).
[21] H. Myalska, G. Moskal, K. Szymański, Surf. Coat. Techn. **260**, 303 (2014).

Received: 20 April 2014.